

11-20-2004

# Estimating the sliding velocity of a Pleistocene ice sheet from plowing structures in the geologic record

Neal R. Iverson  
*Iowa State University*, niverson@iastate.edu

Thomas S. Hooyer  
*University of Wisconsin-Madison*

Follow this and additional works at: [http://lib.dr.iastate.edu/ge\\_at\\_pubs](http://lib.dr.iastate.edu/ge_at_pubs)



Part of the [Glaciology Commons](#), and the [Sedimentology Commons](#)

The complete bibliographic information for this item can be found at [http://lib.dr.iastate.edu/ge\\_at\\_pubs/141](http://lib.dr.iastate.edu/ge_at_pubs/141). For information on how to cite this item, please visit <http://lib.dr.iastate.edu/howtocite.html>.

---

This Article is brought to you for free and open access by the Geological and Atmospheric Sciences at Iowa State University Digital Repository. It has been accepted for inclusion in Geological and Atmospheric Sciences Publications by an authorized administrator of Iowa State University Digital Repository. For more information, please contact [digirep@iastate.edu](mailto:digirep@iastate.edu).

## Estimating the sliding velocity of a Pleistocene ice sheet from plowing structures in the geologic record

Neal R. Iverson

Department of Geological and Atmospheric Sciences, Iowa State University, Ames, Iowa, USA

Thomas S. Hooyer

Wisconsin Geological and Natural History Survey, University of Wisconsin, Madison, Wisconsin, USA

Received 11 February 2004; revised 25 August 2004; accepted 20 September 2004; published 20 November 2004.

[1] As an ice sheet slides over its sediment bed, some clasts partly embedded in the glacier sole plow through the bed surface. The size distribution of such clasts, if it can be characterized from structures in the geologic record, can be used to estimate the sliding velocity of a past ice sheet. By combining a theory of glacier sliding with a geotechnical theory of cone penetration, sliding velocity can be calculated in terms of clast-size parameters, a fluidity parameter for ice, and the thermodynamic properties of ice and clasts. If frictional properties of the bed are measured, the effective normal stress on the bed and bed shear strength during glaciation can also be calculated. We used this approach to estimate the sliding velocity of an Illinoian ice sheet that left plowing structures in cemented outwash near Peoria, Illinois. Fluidity parameters for normal and basal temperate ice yielded sliding velocities of 140–168 m yr<sup>-1</sup> and 60–72 m yr<sup>-1</sup>, respectively. These are overestimates if solutes impeded regelation of ice past clasts or if friction between debris-laden ice and clasts retarded slip. Preconsolidation stresses determined in laboratory tests on silt from the bed agree with effective normal stresses calculated using clast-size parameters. The high shear strength of the bed (>145 kPa) and primary structures preserved within it indicate that additional movement due to pervasive shear of the bed was unlikely. Application of this method elsewhere would provide basal velocity data that are otherwise unavailable for testing and tuning of ice sheet models. *INDEX TERMS*: 1815 Hydrology: Erosion and sedimentation; 1824 Hydrology: Geomorphology (1625); 1863 Hydrology: Snow and ice (1827); *KEYWORDS*: glacier, sliding velocity, plowing, bed deformation, preconsolidation

**Citation:** Iverson, N. R., and T. S. Hooyer (2004), Estimating the sliding velocity of a Pleistocene ice sheet from plowing structures in the geologic record, *J. Geophys. Res.*, 109, F04006, doi:10.1029/2004JF000132.

### 1. Introduction

[2] Fast-flowing ice streams likely contributed to climate variability during the Pleistocene by affecting the dynamics and mass balance of ice sheets [e.g., Clark *et al.*, 1999]. Fast flow usually results from rapid movement at glacier beds. Thus ice sheet models that seek to explain glacier-climate interactions should include such movement and its activation by high basal water pressure [e.g., Clarke *et al.*, 1999]. Although model parameterizations of basal processes include increasing realism [e.g., Marshall and Clarke, 1997a], uncertainties in modeling subglacial hydrology, in particular, preclude accurate assessment of basal velocity. Thus an independent means of estimating basal velocity would be useful for evaluating and tuning models of past ice sheets.

[3] One approach is to use information stored in exposed glacier beds. Grain sizes and structures in the geologic record are used commonly to infer flow regimes of rivers

[e.g., Bradley and Mears, 1980; Costa, 1983], but analogous inferences for glaciers are more problematic due to the large effective viscosity of ice and resultant inhibition of selective particle transport and deposition. Some authors have suggested that the magnitude of elongation of subglacial bed forms is an indicator of sliding velocity [Stokes and Clark, 2002]. This argument, however, depends on two uncertain assumptions: that elongation is controlled by the magnitude of ice displacement, rather than by the overall strain field of the basal ice, and that displacement magnitude depends primarily on sliding velocity, rather than on the duration of glacier occupation. Even if these assumptions are taken at face value, bed form elongation does not provide a quantitative estimate of velocity. To date, therefore, exposed glacier beds have yielded information only on the kinematics of basal movement, with no information on basal velocity.

[4] Herein we use structures in sediments of a pre-Wisconsin advance of the Lake Michigan lobe to estimate the lobe's sliding velocity. The structures allow measurement of the size distribution of clasts that plowed through

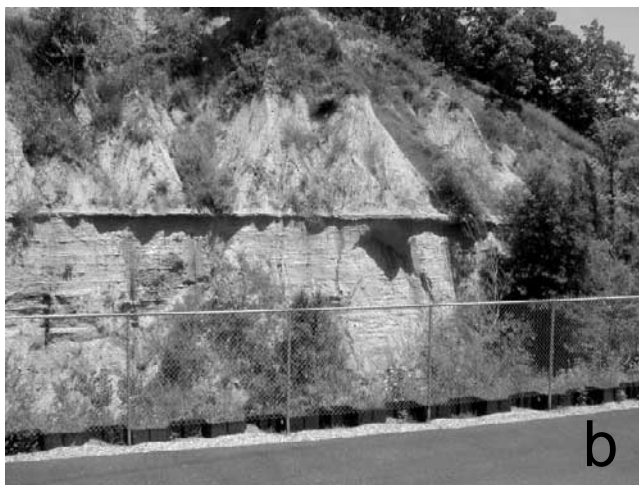
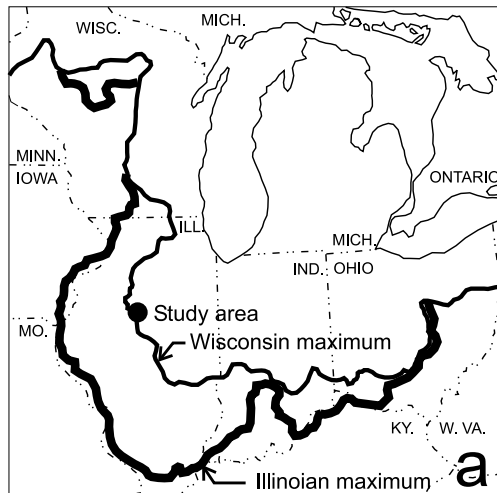


**Figure 1.** (a) Location of study area and limits of the Wisconsin and Illinoian ice sheets [modified from *Prior, 1991*]. (b) Radnor till overlying stratified sand and gravel at the Glendale School section. The cemented zone at the upper surface of the sand and gravel is clearly visible as a resistant layer, above the top of the fence. The upper surface of the cemented zone contains the plowing structures.

the bed surface during sliding. This size distribution, when analyzed by combining a theory of glacier sliding [*Lliboutry, 1979*] with a geotechnical theory of cone penetration [*Seneset and Janbu, 1985*], yields the sliding velocity, effective normal stress on the bed, and bed shear strength in terms of only a few parameters that are known independently. Preconsolidation tests on bed sediments allow limited testing of the analysis.

## 2. Measurements

[5] In East Peoria, Illinois, ~8 m of till of the Radnor member of the Illinoian Glasford Formation overlies horizontally stratified sand and gravel in what is locally called the Glendale School section (Figures 1a and 1b) [*Follmer et al., 1979*]. The thickness of the sand and gravel is unknown, but more than 8 m is exposed in the section. The exposure occurs along the steep northern valley wall of a tributary of

Farm Creek (SE NW NE Sec. 3, T. 25 N. R. 4W, Tazewell Co., Illinois, Peoria East, 7.5 min quadrangle). The Sangamon paleosol developed at the upper surface of the till establishes that these sediments predate the last glaciation. Overlying the Radnor till is ~6 m of Wisconsin-age loess (Roxana and Peoria Silt) and till (Wedron Formation) [*Hansel and Johnson, 1996*].

[6] *Clark and Hansel* [1989] described in detail the contact between the base of the Radnor till and underlying sand and gravel, which they interpreted to be outwash. About 0.01–0.02 m of till above this contact and 0.2–0.3 m of sand and gravel below it have been lithified by carbonate cementation (Figure 1b). The source of the carbonate was probably the till, which is calcareous (22–27%). Thus cementation occurred after, rather than during, slip of ice over the outwash. However, cementation could have occurred subglacially shortly after accretion of the till began, owing to diffusion of CO<sub>2</sub> from descending glacial meltwater as it moved from the till to the better aerated sand and gravel [*Clark and Hansel, 1989*]. The cemented contact is difficult to access in situ because it outcrops more than 6 m up the steep valley wall and is overlain by ~14 m of sediment (Figure 1b). However, slabs of the cemented zone (0.25–10 m<sup>2</sup>) have fallen from the outcrop and provide easy access to ~20 m<sup>2</sup> of the former bed.

### 2.1. Size Distribution of Clasts That Plowed

[7] As a wet-based glacier slips over a sediment bed, clasts at the bed surface that are partially embedded in the glacier sole can be pushed through the sediment: a process called plowing [e.g., *Brown et al., 1987; Clark and Hansel, 1989; Alley, 1989*]. Plowing clasts eventually either lodge or are plucked from the bed by sliding ice.

[8] Observations of the cemented contact leave little doubt that this process occurred as the ice sheet slipped over the sand and gravel outwash in this area [*Clark and Hansel, 1989*]. Two structures indicative of plowing are ubiquitous: ridges of sediment, called prows, and grooves (Figure 2). Prows occur immediately adjacent to clasts (Figure 2a), or to the former positions of clasts (Figure 2b), and tend to be crescent shaped in plan view. They usually do not extend from the clast more than one clast diameter. Prows sometimes extend to the tops of clasts but more commonly extend only partway up the clast surface from the mean level of the bed (Figure 2a). Smaller particles within the prows tend to be oriented parallel with the clast surface [*Clark and Hansel, 1989, Figure 3*], consistent with compression normal to the edge of the clast. Grooves (Figures 2a and 2c) extend from clasts in the opposite direction from prows. Lengths of grooves may exceed 1 m, and their widths correspond to the sizes of associated clasts. Some grooves are curved in plan view (Figure 2a), but most are straight (Figure 2c).

[9] These observations are strong evidence that clasts were pushed through the glacier substrate, resulting in bulldozing of the bed that caused both prow formation down-glacier from clasts and grooves up-glacier. Striations on some of the larger clasts are generally parallel to the grooves but diverge on the up-glacier sides of clasts and converge on their down-glacier sides (Figure 2a). This observation reinforces the viewpoint that sliding ice dragged clasts through the bed.

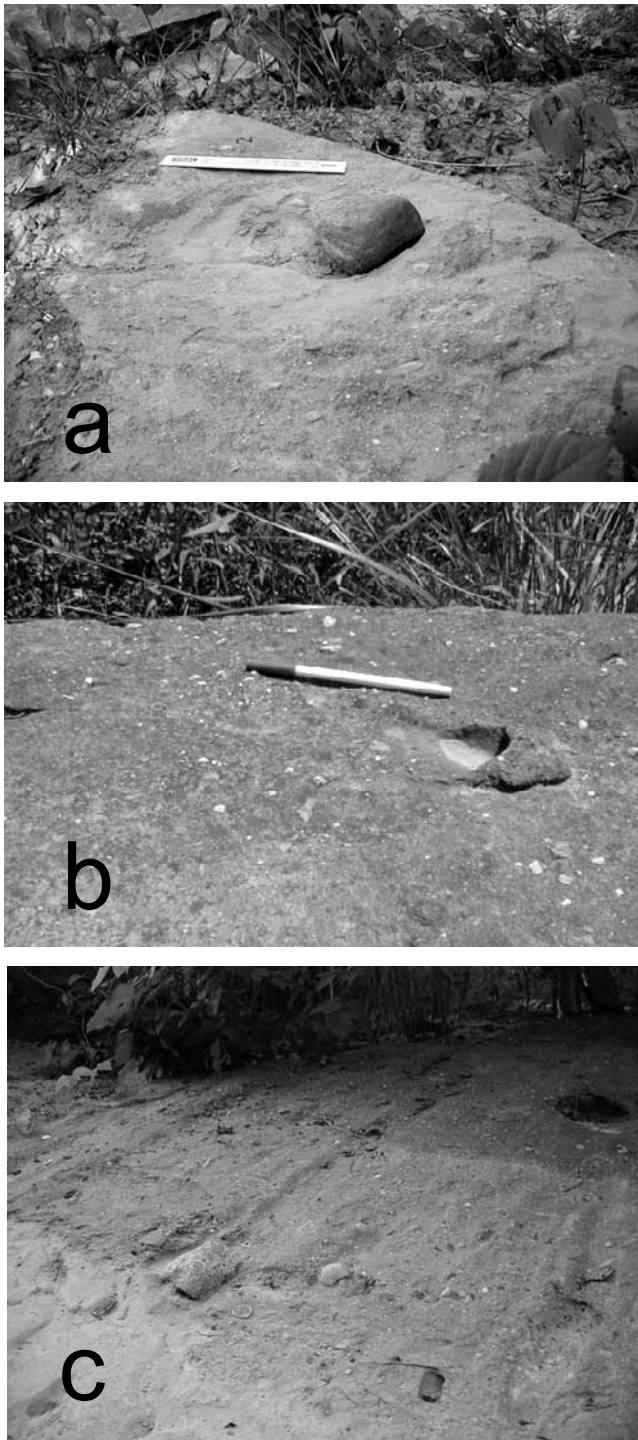


**Figure 2.** (a) Large clast that has plowed from left to right, with prow and groove. The ruler is 0.3 m long. (b) Well-developed prow with clast absent. Plowing was from left to right. (c) Grooves formed by clast plowing from upper right to lower left. The largest clast (at lower left) is  $\sim 0.09$  m long.

[10] Our hypothesis is that the size distribution of clasts that have plowed can be used to estimate sliding velocity. We measured the sizes of clasts with associated prows and grooves over  $18.4 \text{ m}^2$  of slabs that had fallen from the outcrop. Not all clasts had both prows and grooves, but either a prow or groove was considered evidence of plowing. Sizes of clasts were determined by measuring the lengths of their longest and shortest principal axes and averaging those lengths. The clast responsible for prows and grooves was sometimes absent (Figure 2b). In this case the groove width and the geometry of the prow were used to estimate two of the clast dimensions, which were then averaged.

[11] A total of 121 instances of plowing were identified, and in 62 of these cases, both prows and grooves were identified. The size distribution of clasts that plowed is shown in Figure 3a. Three aspects of this distribution are of interest: (1) no clasts with mean diameters smaller than  $\sim 8$  mm plowed, despite observations of hundreds of smaller particles at the former bed surface; (2) large numbers of

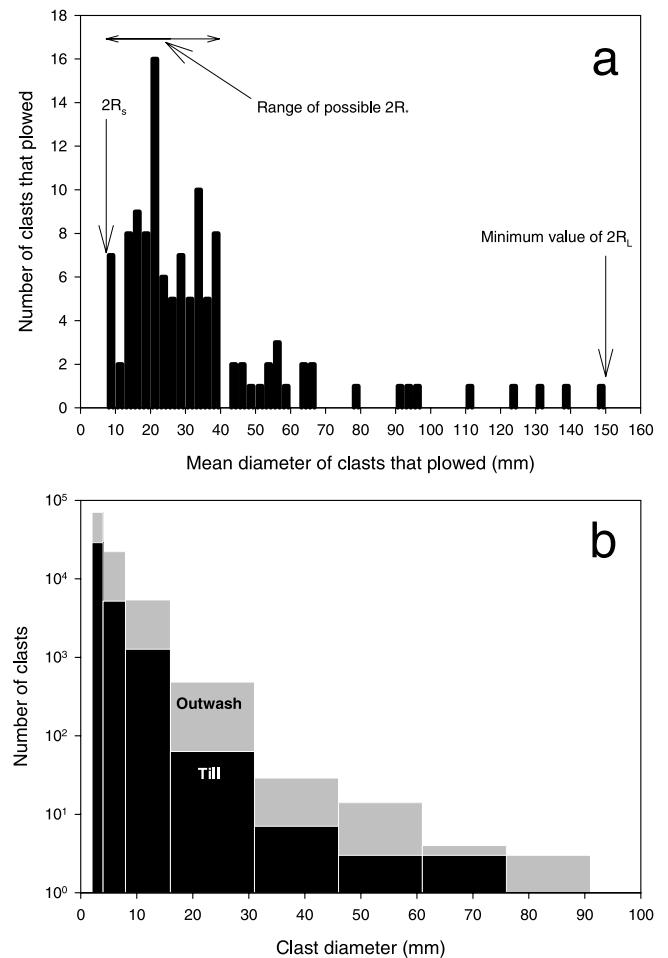


**Figure 3.** (a) Number of clasts that plowed as a function of their size. Symbols for variables are defined in text. (b) Number of clasts in outwash and till samples ( $\sim 32$  L each) as a function of clast size. The numbers of particles  $< 16$  mm in diameter were determined by counting a representative fraction of the total mass in each size range.

clasts between 8 and 40 mm in diameter plowed; and (3) no clast plowed that was larger than 148 mm.

[12] Glacier-sliding theory provides a general explanation for these observations. A clast plows if the drag exerted on it by ice is sufficient to equal the yield resistance of the substrate. The drag, equal to the local shear stress on the clast, depends on the combined action of regelation and enhanced creep of ice past clasts. These processes depend on clast size. Ice moves with minimal drag past sufficiently small clasts primarily by regelation and with minimal drag past sufficiently large clasts primarily by enhanced creep. For clasts of an intermediate size, analogous to the transition wavelength of sliding theory [Paterson, 1994, p. 142], regelation and enhanced creep contribute equally to the drag on clasts, and the total drag is maximized. Thus clasts smaller and larger than threshold sizes do not plow because the drag urging them forward is too small. Clasts near the transition size, subject to the maximum drag, are most likely to plow.

[13] These tenets of sliding theory are consistent with the measured clast-size distribution, with its lower and upper size thresholds and intermediate sizes for which plowing was common (Figure 3a). Interpreting the data, however, is complicated by the unequal probability of clasts of different sizes at the bed surface: larger clasts are less common. In principle, the data could be normalized to the size distribution of the source of the clasts. That source, however, could be either the sediment of the glacier, represented by the overlying till, or the outwash of the glacier bed. Thus a meaningful way to normalize the number of clasts that plowed to the number of clasts available is not clear.

[14] Despite this ambiguity, some solid interpretations are possible from the measured clast-size distribution. The lower size threshold (8 mm) must reflect low bed-parallel drag on small clasts because hundreds of smaller particles were observed that did not plow. One explanation for the low drag would be a layer of water between the ice and the bed that drowned particles smaller than the lower size threshold. A water layer several millimeters thick, however, would have been unlikely due to the high transmissivity of the sand and gravel substrate and the instability of thick water layers even in the presence of an impermeable bed [Walder, 1982]. Moreover, fine sorted sediment would have been transported in a thick water layer at the outwash-till contact, and there is no evidence of such sediment. Thus the lower size threshold likely reflects the ease of ice regelation past small clasts. The upper size threshold is less certain due to the relative scarcity of cobbles and boulders. Nevertheless, clasts as large as 148 mm did plow, so this diameter is a minimum value for the upper size threshold. Also, owing to the scarcity of larger clasts, the transition clast size cannot be specified exactly from Figure 3a. However, a conservative interpretation is that this clast size was between 8 mm, the lower bound of the size range with the smallest clasts that plowed, and 40 mm, above which there was an abrupt reduction in the number of clasts that plowed (Figure 3a). No similarly abrupt reduction was apparent in the bulk grain-size distributions of either the till or outwash, although particle number decreases dramatically as size increases (Figure 3b). Thus in our analysis we assume that (1) clasts <8 mm in diameter could not plow because drag

on them exerted by sliding ice was too small, (2) clasts at least as large as 148 mm were subject to drags sufficient to cause plowing, and (3) clasts of the transition size subject to the highest drag were between 8 and 40 mm in diameter.

## 2.2. Preconsolidation Stresses

[15] Whether clasts plow at a particular sliding velocity depends on the yield strength of the bed. In granular Coulomb materials this yield strength depends on the effective normal stress, which is equal to the difference between the total normal stress on the bed and the pore-water pressure. We conducted laboratory tests on sediment of the bed to measure its preconsolidation stress, the largest effective normal stress sustained by the sediment since its deposition.

[16] Water-saturated confined sediment subjected to a load will contract if water can escape from pores. At small stresses, contraction will be primarily elastic and hence recoverable if the stress is removed. However, if stress exceeds previous stresses on the sediment, contraction will be permanent. The stress at which sediment begins to contract permanently is the preconsolidation stress. It is a measure of the maximum effective normal stress because only the largest stress sets the value required for initiating further permanent deformation. Preconsolidation stresses of basal tills have been measured commonly, usually by obtaining intact till specimens and loading them incrementally in a consolidometer [e.g., Harrison, 1958; Larsen *et al.*, 1995].

[17] Using this approach, we sampled cohesive, laminated silt lenses within the sand and gravel of the former bed. The lenses are about a decimeter thick and 1–2 m long. Sediment above the silt lenses was excavated, and samples of the silt were obtained several decimeters in from the outcrop face. Samples (75 mm diameter and 20 mm thick) were collected, minimizing disturbance of the specimen [Hooyer and Iverson, 2002].

[18] Specimens were inserted in a fixed-ring consolidometer, saturated with water, and loaded incrementally following a standard procedure [Das, 1994, p. 250]. Values of preconsolidation stress were determined using the method of Casagrande [1936], summarized by Hooyer and Iverson [2002, Appendix 1].

[19] Consolidation curves for five specimens are shown in Figure 4, with corresponding values of preconsolidation stresses (two other specimens were collected, but testing problems prevented obtaining preconsolidation stresses). The mean value was 1160 kPa, with a standard deviation of 555 kPa. As expected, preconsolidation stresses exceeded the present normal stress on the silt lenses exerted by the weight of overlying sediment.

[20] A couple of factors complicate interpretation of these data. Although specimens were collected away from the face of the outcrop and well below where pedogenic processes may have disturbed the sediment, the specimens were drier than during glaciation. Such drying can cause consolidation of fine-grained sediments, yielding preconsolidation stresses that are too large [Mickelson *et al.*, 1979; Tulaczyk *et al.*, 2001]. In addition, Wisconsin-age till overlies the Illinoian sediment of this study, so preconsolidation stresses may reflect loading during the more recent glaciation. Thus a conservative interpretation is that effective

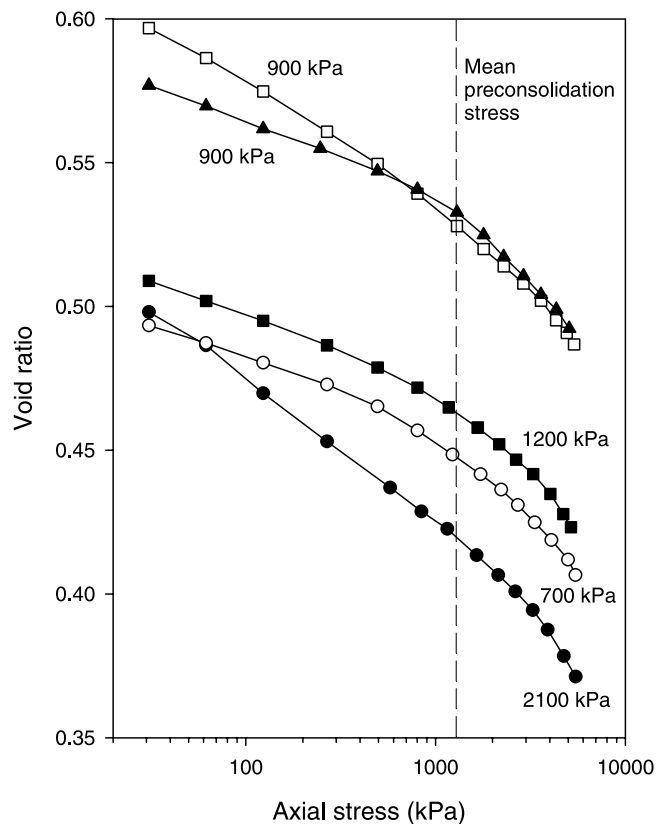


**Figure 4.** Results of preconsolidation tests on five specimens of fine-grained sediment (mostly silt) collected from the bed. Preconsolidation stresses are shown for each specimen. The variation in initial void ratio likely reflects textural differences among specimens.

normal stresses did not exceed measured preconsolidation stresses but may have been smaller.

### 3. Analysis

[21] In order to use the size distribution of clasts that plowed (Figure 3a) to estimate basal velocity, we first distinguish the velocity of plowing clasts from the sliding velocity at the bed surface. The sediment bed, which normally has some frictional strength, resists clast motion. Thus clasts move at a velocity,  $U_p$ , that is less than the sliding velocity,  $U$ , such that there is a relative velocity,  $U_r$ , between clasts and the ice:

$$U_r = U - U_p. \quad (1)$$

[22] Consider now the bed geometry used in plowing analyses [Brown *et al.*, 1987; Alley, 1989; Iverson, 1999] in which clasts are idealized as spheres centered at the ice-bed interface (Figure 5a). Observations of clasts (Figure 2) indicate that this is a better idealization than the subdued sinusoidal bumps that have also been considered [Brown *et al.*, 1987; Iverson, 1999]. Real clasts, of course, are neither spherical nor necessarily centered on the bed, but in considering a large number of clasts, a spherical, bed-centered clast is a reasonable average geometry. The sliding

velocity of ice past the upper surfaces of clasts during plowing is best analyzed with the theory of Lliboutry [1979], who considered flow of temperate ice past isolated hemispheres. Retaining his notation, for the ice rheology of Glen (stress exponent of 3) and the case of no ice-clast separation,

$$U_r = B_1 \tau^3 R + C_1 \tau / R, \quad (2)$$

where  $R$  is the clast radius,  $\tau$  is the shear stress (bed-parallel force/ $\pi R^2$ ) on the clast,  $B_1$  is a fluidity parameter for ice, and  $C_1$  is a regelation parameter. The first and second terms on the right-hand side are the velocity components due to enhanced creep and regelation, respectively. Following Lliboutry [1979, Table 1],  $B_1 = A/42.6$ , where  $A$  is the ice fluidity parameter in the most common writing of Glen's flow rule [Paterson, 1994, p. 85]. The regelation parameter depends on the lowering of the melting temperature of ice per unit pressure,  $C$ , the volumetric latent heat of fusion of ice,  $L_v$ , and the thermal conductivities of temperate ice,  $K_i$ , and clasts,  $K_r$  [Lliboutry, 1979, Table 1]:

$$C_1 = \frac{3C(K_r + 2K_i)}{L_v}. \quad (3)$$

[23] Whether there were water-filled cavities adjacent to the down-glacier surfaces of clasts is potentially important. If sediment prows, pushed upward by plowing, filled such

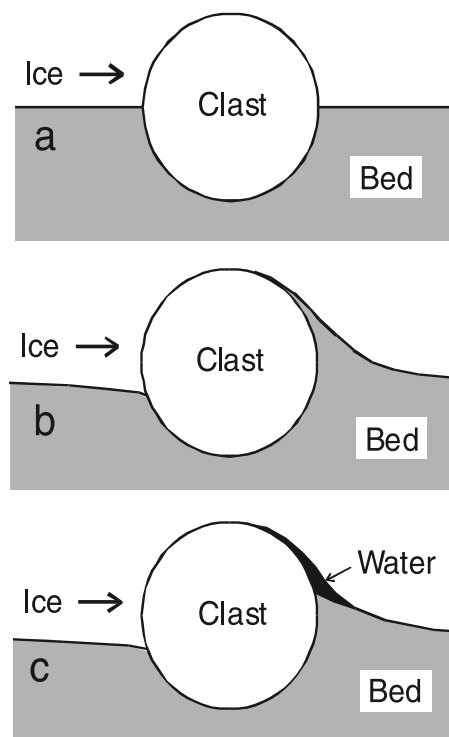


**Figure 5.** (a) Idealization of a plowing clast. (b) Plowing clast with till intruding into the zone of low ice pressure down-glacier from the clast. (c) Plowing clast with less till intrusion and a water-filled cavity.

**Table 1.** Parameter Values for Calculating Sliding Velocity

Parameter	Symbol	Value	Source
Ice fluidity parameter	$B_1$	$1.6 \times 10^{-25} \text{ Pa}^{-3} \text{ s}^{-1}$ (normal ice) $8.7 \times 10^{-25} \text{ Pa}^{-3} \text{ s}^{-1}$ (basal ice)	<i>Lliboutry and Duval</i> [1985] <i>Cohen</i> [2000]
Melting temperature depression	$C$	$7.4 \times 10^{-8} \text{ K Pa}^{-1}$	<i>Paterson</i> [1994]
Regelation parameter	$C_1$	$2.66 \times 10^{-15} \text{ m}^2 \text{ Pa}^{-1} \text{ s}^{-1}$	this study, <i>Lliboutry</i> [1979]
Sediment cohesion	$c$	0 kPa	this study (direct-shear tests)
Ice thermal conductivity	$K_i$	$2.1 \text{ W m}^{-1} \text{ K}^{-1}$	<i>Paterson</i> [1994]
Rock thermal conductivity	$K_r$	$3.0 \text{ W m}^{-1} \text{ K}^{-1}$	<i>Touloukian et al.</i> [1981]
Pressure-shadow factor	$k$	0.1–0.45	<i>Brown et al.</i> [1987]
Ice volumetric latent heat of fusion	$L_v$	$3 \times 10^{-8} \text{ J m}^{-3}$	<i>Paterson</i> [1994]
Modified bearing capacity factor, no cavities	$N$	2.09–6.66	this study (equation (7))
Modified bearing capacity factor, with cavities	$N_c$	3.72–15.55	this study (equation (8))
Bearing capacity factor	$N_F$	26–40	<i>Senne set and Janbu</i> [1985]
Radius of smallest clast that plowed	$R_s$	0.004 m	this study (field data)
Radius of largest clast that plowed	$R_L$	>0.074 m	this study (field data)
Transition clast radius	$R_*$	0.017–0.020 m	this study (field data/equation (14))
Sediment friction angle	$\phi$	$35^\circ$	this study (direct-shear tests)
Sliding constant	$\Psi$	$3.43 \times 10^{-10} \text{ m}^3 \text{ s}^{-1}$ (normal ice) $1.47 \times 10^{-10} \text{ m}^3 \text{ s}^{-1}$ (basal ice)	this study (equation (11)) this study (equation (11))

cavities (Figure 5b), then the sediment would effectively be a down-glacier extension of the clast such that (2) would be a good approximation. Alternatively, it is possible that cavities were too thin to be occupied by sediment such that they were filled with only water under a pressure controlled by the basal hydrological system (Figure 5c). *Lliboutry* [1979] considered water-filled cavities. He assumed that cavities did not affect stresses on up-glacier surfaces and that ice separated from the full down-glacier half of hemispheres. The shear stress on a clast,  $\tau_c$ , is then

$$\tau_c = \frac{1}{2}(\tau + P_e), \quad (4)$$

where  $P_e$  is the effective normal stress on the bed, defined as the difference between the ambient normal stress on the bed and the water pressure [*Lliboutry*, 1979, equation (47); *Iverson*, 1999, Appendix].

[24] Geotechnical studies in which cones and piles are driven downward through sediment [e.g., *Verruijt et al.*, 1982; *Chaney and Demars*, 1985] provide the basis for estimating the magnitude of the resistive shear stress that the bed exerts up-glacier on plowing clasts. *Iverson* [1999] used the penetration model of *Senne set and Janbu* [1985], which is applicable to plowing elements of different shapes, to estimate this shear stress,  $\tau_p$ :

$$\tau_p = \frac{1}{2 + N_F k} \left[ N_F \left( P_e + \frac{c}{\tan \phi} \right) - \frac{c}{\tan \phi} \right]. \quad (5)$$

The pressure-shadow factor,  $k$ , accounts for flow of ice past clasts and the resultant less-than-ambient total normal stress on the bed immediately down-glacier;  $\phi$  is the friction angle of the bed sediment;  $c$  is its cohesion;  $N_F$  is a dimensionless bearing capacity factor that depends on the frictional properties of the sediment and the shape of the plowing element [*Iverson*, 1999, equation (13)]. Note that  $\tau_p$  is independent of particle size and velocity. Empirical support for the *Senne set and Janbu* [1985] model is discussed by *Iverson* [1999]. The value of  $k$  depends on whether regelation or creep dominates ice motion past clasts [*Brown et al.*, 1987] and can be calculated from sliding theory.

Other parameters in (5), except for  $P_e$ , can be measured in laboratory tests.

[25] Fully drained Coulomb behavior for the sediment is assumed in (5) such that shear stress is independent of plowing velocity and dependent on effective normal stress. This assumption is overwhelmingly supported by cone penetration studies in coarse-grained sediments. In sediments that contain significant silt and clay, however, excess pore pressures may occur. Pore pressure diffusion in such sediment beneath the cone cannot keep pace with the rate of compaction there, resulting in excess pore pressures that decrease drag on the cone as its speed increases [*Campanella et al.*, 1983]. Scaling arguments [*Iverson*, 1999], tested using laboratory plowing experiments with hemispheres [*Thomason and Iverson*, 2003], indicate ranges of plowing speed and sediment permeability and compressibility over which significant excess pore pressures are likely to develop. For the permeable and relatively incompressible sand and gravel bed of this study, excess pore pressures can be neglected; they would be significant only at plowing speeds orders of magnitude larger than the highest speeds of glaciers.

[26] To satisfy quasi-static stress equilibrium, the down-glacier shear stress exerted by sliding ice on plowing clasts must equal the shear stress exerted up-glacier by the yielding sediment bed. For the case of no water-filled cavities down-glacier from clasts, this requires that  $\tau = \tau_p$ . Substituting (5) into (2) and requiring that  $c = 0$  for the sand and gravel bed yields

$$U_r = B_1 P_e^3 N^3 R + C_1 P_e N / R, \quad (6)$$

where  $N$  is dimensionless and given by

$$N = \frac{N_F}{2 + N_F k}. \quad (7)$$

For the case of water-filled cavities,  $\tau_c = \tau_p$ , and from (4),  $\tau = 2\tau_c - P_e$ . Substituting (5), set equal to  $\tau_c$ , into this equation and the result into (2) yields an equation with the same form as (6) but with  $N$  replaced by an analogous

dimensionless parameter appropriate for the case of water-filled cavities,  $N_c$ :

$$N_c = \frac{N_F}{1 + \frac{1}{2}N_F k} - 1. \quad (8)$$

[27] Although (6) is of limited value because  $P_e$  for past glacier beds is seldom known independently,  $P_e$  can be determined if the transition clast radius,  $R_*$ , is known.  $U_r$  will be minimized for clasts of this size because drag stresses on such clasts are maximized. Thus for  $R = R_*$ ,  $dU_r/dR = 0$ . Differentiating the right-hand side of (6) with respect to  $R$ , setting the result equal to zero, and substituting  $R = R_*$  yields

$$P_e = \left(\frac{C_1}{B_1}\right)^{\frac{1}{2}} \frac{1}{NR_*} \quad (9)$$

in the absence of water-filled cavities. For the case of water-filled cavities,  $N$  in (9) is replaced by  $N_c$ . Thus  $P_e$  for both cases is a simple function of the transition clast size and material properties of the ice and bed. Substituting (9) into (6) allows  $U_r$  to be expressed in terms of  $R_*$  rather than  $P_e$ :

$$U_r = \Psi \left( \frac{R}{R_*^3} + \frac{1}{RR_*} \right), \quad (10)$$

where

$$\Psi = \left( \frac{C_1^3}{B_1} \right)^{\frac{1}{2}}. \quad (11)$$

$U_r$  depends inversely on  $B_1$ , which is counterintuitive. The inverse dependence results from the nonlinear rheology of ice, which causes its effective viscosity to decrease with increasing  $U_r$ . Note that (10) applies regardless of whether there were water-filled cavities down-glacier from clasts.

[28] The absolute sliding velocity,  $U$ , can be determined from (10) if the radii of the largest and smallest clasts that plowed are known. Multiplying both sides of (10) by  $R$  yields a quadratic equation in  $R$ . The two roots of this equation have special significance as  $U_p$  approaches zero and  $U_r$  approaches  $U$  in (1). The roots, in this case, correspond to the radii of the smallest and largest clasts that plowed. For these threshold clast sizes the drag necessary to move clasts is attained only if  $U_r$  is essentially equal to but infinitesimally smaller than  $U$ .  $U_p$ , in this case, is thus very small but nonzero. Defining  $R_s$  and  $R_L$  as the radii of the smallest and largest clasts that plowed and setting  $U_r = U$  in (10) provides  $U$  as functions of  $R_s$  and  $R_L$ :

$$U = \Psi \left( \frac{R_s}{R_*^3} + \frac{1}{R_s R_*} \right) \quad (12)$$

$$U = \Psi \left( \frac{R_L}{R_*^3} + \frac{1}{R_L R_*} \right). \quad (13)$$

Sliding velocity, therefore, can be estimated with only the size distribution of clasts that plowed and the properties of ice and rock contained in  $\Psi$  (equation (11)). Values of  $R_s$ ,  $R_L$ , and  $R_*$  will usually be imperfectly known from field observations, as in this study. These values can be better constrained by equating the right-hand sides of (12) and (13) to obtain

$$R_* = (R_s R_L)^{\frac{1}{2}}. \quad (14)$$

Field determinations of the values of  $R_s$ ,  $R_L$ , and  $R_*$  should satisfy (14). Substituting (14) into either (12) or (13) to eliminate  $R_*$  yields  $U$  in terms of  $R_s$  and  $R_L$ :

$$U = \frac{\Psi}{(R_L R_s)^{\frac{1}{2}}} \left( \frac{1}{R_L} + \frac{1}{R_s} \right). \quad (15)$$

Thus (12), (13), or (15) can be used to estimate sliding velocity, provided that two of the parameters  $R_s$ ,  $R_L$ , and  $R_*$  are known.

[29] Although the sliding velocity at the ice bed interface can be estimated using this approach, a final consideration is whether additional motion occurred as a result of pervasive shear of the bed [e.g., *Boulton and Hindmarsh*, 1987]. For such deformation to occur the shear stress on the bed must equal its yield strength in shear,  $S$ , given by the Coulomb yield criterion:  $S = P_e \tan \phi + c$ . The value of  $S$  can be determined readily because  $P_e$  is given by (9), and  $c = 0$  for the sand and gravel bed. Substituting (9) into the Coulomb criterion with  $c = 0$  yields

$$S = \left( \frac{C_1}{B_1} \right)^{\frac{1}{2}} \frac{\tan \phi}{NR_*} \quad (16)$$

if there are no water-filled cavities. Substituting  $N_c$  for  $N$  in (16) yields  $S$  if cavities are present. The value of  $S$  calculated from (16) can be compared with shear stresses on beds of modern glaciers to determine whether pervasive shear of the bed was likely.

#### 4. Results

[30] To estimate sliding velocity, the material constants ( $C_1$  and  $B_1$ ) that constitute  $\Psi$  must be known. We use  $B_1 = 1.60 \times 10^{-25} \text{ Pa}^{-3} \text{ s}^{-1}$ , commensurate with  $A = 6.82 \times 10^{-24} \text{ Pa}^{-3} \text{ s}^{-1}$ , the value of the flow law parameter suggested by *Lliboutry and Duval* [1985], for clean, temperate ice that is isotropic with an intermediate water content. This is the same value advocated by *Paterson* [1994, p. 97]. For clean temperate ice, (3) indicates that  $C_1 = 2.66 \times 10^{-15} \text{ m}^2 \text{ Pa}^{-1} \text{ s}^{-1}$ . Values of parameters used to compute  $C_1$  and of the other variables used to calculate sliding velocity are listed in Table 1.

[31] Figure 6 illustrates sliding velocity as a function of  $R_s$  and  $R_L$ , as indicated by (15). Smaller values of  $R_s$  imply higher sliding velocities because a higher velocity is necessary to move a clast if it is small and easily accommodated by regelation. For a given value of  $R_s$ , sliding velocity decreases with increasing  $R_L$ . Physically, this results from the nonlinear flow relation for ice. The consequent inverse relation between effective ice viscosity and sliding velocity



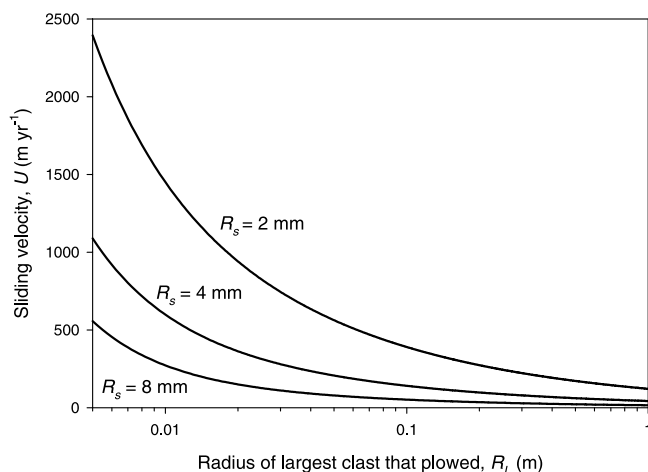


**Figure 6.** Sliding velocity as a function of  $R_L$  for different values of  $R_s$  and for normal temperate ice (clean, isotropic, intermediate water content).  $R_s = 4$  mm is the value indicated by plowing structures.

causes  $R_*$  [Lliboutry, 1979, equation (45)] and hence  $R_L$  (see (14)), to be inversely related to sliding velocity.

[32] To estimate sliding velocity, two of the clast-size parameters ( $R_s$ ,  $R_L$ , and  $R_*$ ) must be known. The absence of clasts that plowed with diameters  $< 8$  mm indicates that  $R_s = 4$  mm.  $U$  is plotted for this case in Figure 7a as a function of both  $R_L$  and  $R_*$ . The size distribution of clasts that plowed indicates  $R_L > 74$  mm (Figure 3a). Using these values of  $R_s$  and  $R_L$  in (14),  $R_*$  must have been greater than 17 mm. In addition, the distribution of clasts that plowed indicates  $R_* < 20$  mm. Thus  $R_*$  is constrained to a narrow range, 17–20 mm. It is reasonable that this range lies at the upper bound of the permissible values shown in Figure 3a because larger clasts are less common (Figure 3b). The sliding velocity, calculated using  $R_s = 4$  mm and  $R_* = 17$ –20 mm in (12), is 140–168 m yr<sup>-1</sup> (Figure 7a).

[33] This analysis can be tested, to a limited extent, by using (9) to calculate the effective normal stress,  $P_e$ , for comparison with the measured preconsolidation stress. This requires determining values of  $N$  and  $N_c$ , corresponding to cases without and with water-filled cavities downstream from clasts, respectively. These factors depend on the pressure-shadow factor,  $k$ , and the bearing capacity factor,  $N_F$ . The value of  $k$  depends on whether regelation or enhanced creep dominated motion past clasts; values of 0.1–0.45 were suggested by Brown *et al.* [1987] based on theory for the end-member cases of only regelation [Nye, 1968] and only enhanced creep [Lliboutry and Ritz, 1978]. We conducted direct shear tests [Lambe and Whitman, 1969, p. 119] on the outwash of the former bed that yielded a friction angle of 35° and  $c = 0$ . This corresponds to  $N_F = 26$ –40 [Senneset and Janbu, 1985, Figure 44]. When used in (7) and (8), these ranges of  $k$  and  $N_F$  yield  $N = 2.09$ –6.66 and  $N_c = 3.72$ –15.55. Considering cases both with and without water-filled cavities and  $R_* = 17$ –20 mm, the possible range of  $P_e$  indicated by (9) is 490–3630 kPa. The measured preconsolidation stress was  $1160 \pm 555$  kPa, so the range of  $P_e$  indicated by (9) is consistent with the

preconsolidation stress. The associated bed shear strength indicated by (16) is 340–2540 kPa.

[34] Although we have assumed that ice at the bed was “normal” glacier ice, basal ice is usually dirty, with crystalline anisotropy and abnormally high water content, all of which may weaken ice. Therefore the fluidity parameter,  $B_1$ , may have been larger than assumed. Rather than attempt to quantify the individual effects of debris, fabric, and water content on  $B_1$ , we consider the value of  $B_1$  determined in situ at the bed of Engabreen, a temperate glacier in Norway [Cohen, 2000]. An obstacle was inserted in sliding basal ice with 3–17% debris by volume and water content  $> 2\%$ . The drag on the obstacle and sliding velocity were measured; finite element modeling of flow around the obstacle yielded the mean value  $B_1 = 8.7 \times 10^{-25} \text{ Pa}^{-3} \text{ s}^{-1}$  ( $A = 3.7 \times 10^{-23} \text{ Pa}^{-3} \text{ s}^{-1}$ ). Using the same parameters as before, this value of  $B_1$  yields  $U = 60$ –72 m yr<sup>-1</sup> (Figure 7b), more than a factor of two smaller than for normal ice. For this case,  $P_e = 207$ –1560 kPa, which again agrees with the preconsoli-

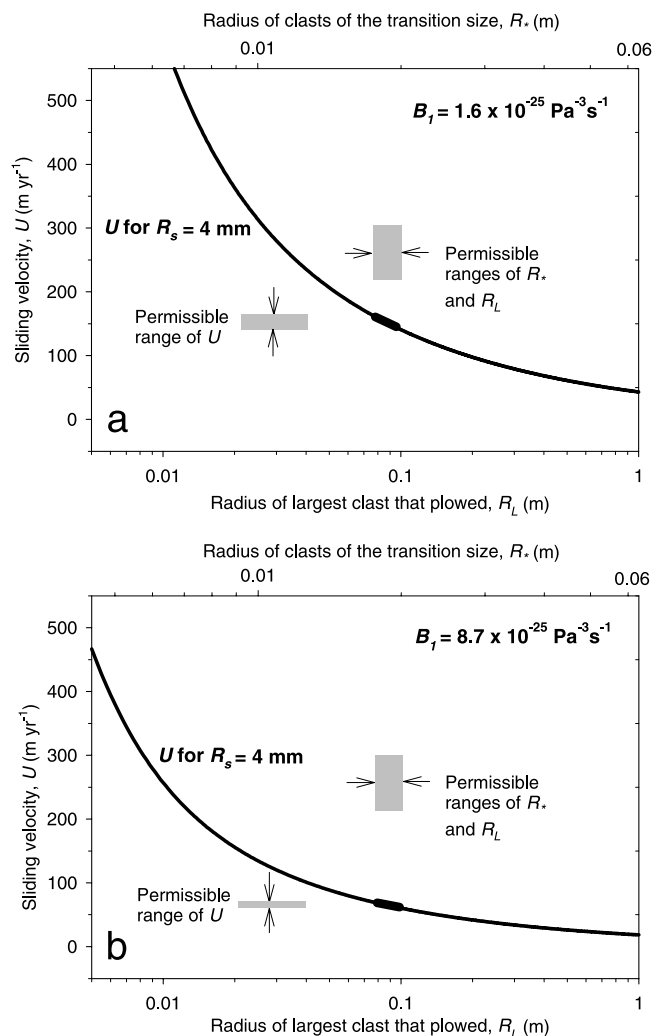


**Figure 7.** Sliding velocity as a function of  $R_L$  and  $R_*$  for  $R_s = 4$  mm and a value of  $B_1$  for (a) normal temperate ice (clean, isotropic, intermediate water content) and (b) basal ice [Cohen, 2000].

**Table 2.** Calculated Parameter Values

Parameter	Normal Temperate Ice ( $B_1 = 1.6 \times 10^{-25} \text{ Pa}^{-3} \text{ s}^{-1}$ )	Basal Temperate Ice ( $B_1 = 8.7 \times 10^{-25} \text{ Pa}^{-3} \text{ s}^{-1}$ )
Sliding velocity, $U$ , $\text{m yr}^{-1}$	140–168	60–72
Effective normal stress, $P_e$ , kPa	490–3630	207–1560
Bed shear strength, $S$ , kPa	340–2540	145–1090

dation stress, and  $S = 145\text{--}1090$  kPa. Table 2 compares values of  $B_1$ ,  $U$ ,  $P_e$ , and  $S$  for normal temperate ice and the basal ice of Engabreen.

## 5. Discussion

[35] This method provides the only technique available for estimating sliding velocity of past ice sheets from their sediments. Arguably, sliding velocity is more important than any other single variable in assessing the dynamics and geomorphic effects of ice sheets. There is clear motivation, therefore, for applying this technique elsewhere by seeking out bedding surfaces in glacial sediments where plowing structures can be identified.

[36] The unusual mechanical properties of the fault where a glacier slips over a sediment bed allow estimation of sliding velocity. The ice hanging wall, as a regelating, viscous fluid, exerts driving stresses on clasts that depend on sliding velocity and clast size. The sand and gravel footwall, as a well-drained Coulomb material, exerts resistive stresses that are independent of plowing velocity and dependent on the effective normal stress and frictional properties of the bed. Clast-size data and bed frictional properties can be determined from the geologic record. There are thus two equations, for driving and resisting stresses, and only two unknowns: the effective normal stress and sliding velocity. The full range of sliding velocity indicated by our measurements, considering both a normal value of  $B_1$  and the higher value appropriate for basal ice, is  $60\text{--}168 \text{ m yr}^{-1}$  (Table 2). This estimate depends only on  $B_1$ ,  $C_1$ , and the clast-size parameters.

[37] Our estimates of effective normal stress on the bed and bed shear strength span broader ranges than our velocity estimates (Table 2) because they depend on whether there were water-filled cavities down-glacier from clasts and on the value of the bearing capacity factor,  $N_F$ , which cannot be specified precisely. For a given bed friction angle,  $N_F$  depends on both the exact shape of the plowing tool and on the degree of sediment compaction. Because neither of these variables is well known, a wide range of  $N_F$  must be adopted ( $N_F = 26\text{--}40$ ). This wide range increases the uncertainties of  $N$  and  $N_c$ , and their different formulations ((compare (7) and (8)) result in the large potential range of effective normal stress and bed shear stress. Our estimates of effective normal stress, although rough, are consistent with the preconsolidation test data, which provide an upper bound for the range of possible effective normal stress.

[38] The calculated shear strength of the bed indicates whether it sheared pervasively at depth. This strength exceeded 145 kPa (Table 2). The largest driving stress for a portion of a modern ice sheet of which we are aware is  $\sim 210$  kPa at Jakobshavn Isbrae, but only part of this stress is supported by the bed [Truffer and Echelmeyer, 2003]. Typical driving stresses for glaciers are  $50\text{--}150$  kPa [Paterson, 1994, p. 240], with basal shear stresses smaller

to varying extents. Thus the sand and gravel bed was likely too strong to deform pervasively in shear. This conclusion is supported by the intact primary stratification of the bed (Figure 1b), including the silt lenses used for the preconsolidation tests; stratification would have been destroyed or disrupted by pervasive shear [e.g., Brown *et al.*, 1987]. Also, this conclusion is supported by the high hydraulic transmissivity of the bed, which was  $>10^{-4} \text{ m}^2 \text{ s}^{-1}$  [Freeze and Cherry, 1979, p. 290]. This aquifer would have favored a gentle hydraulic gradient with low pore water pressure and high effective stress, thereby reducing potential for bed shear [Boulton and Dobbie, 1993]. Thus although Clark and Hansel [1989] rightly emphasized that plowing structures at this site demonstrate the deformable nature of the bed, deformation was limited to the vicinity of plowing clasts where deviatoric stresses were high. Basal movement was focused at the bed surface [e.g., Brown *et al.*, 1987; Hooyer and Iverson, 2002], in contrast to the bed deformation model of glacier flow [e.g., Boulton and Hindmarsh, 1987].

[39] Two potential departures from classical sliding theory, neglected in the analysis, could reduce our estimates of sliding velocity: solutes and friction between debris in ice and clasts. Solutes concentrated down-glacier from clasts where refreezing occurs would lower the melting temperature there. The consequent reduction in heat transfer would impede regelation, as in studies of wire regelation [Drake and Shreve, 1973] and hard-bedded sliding [Hallet, 1976], thereby increasing drags on clasts. The measured size distribution of clasts that plowed could therefore be achieved at a smaller sliding velocity. Estimating the magnitude of this effect is difficult because solute gradients across clasts during plowing are unknown. Nevertheless, the carbonate cementation that preserved the bedding plane indicates that solutes may have been important. In addition, striations on larger clasts indicate that debris in sliding ice was in frictional contact with clasts. This effect, like solutes, would increase drags on clasts so that the clast size distribution would indicate a smaller sliding velocity. Subglacial measurements of the shear traction between debris-charged ice and a smooth rock bed demonstrate that such friction can locally be large ( $>100$  kPa) [Iverson *et al.*, 2003].

[40] Thus an appropriately conservative interpretation of our results is that sliding velocity was less than  $\sim 170 \text{ m yr}^{-1}$  but that, owing to the potential effects of solutes and debris friction, velocity could have been less than the smallest value calculated,  $60 \text{ m yr}^{-1}$ . Archetypes of modern ice streams (Whillans ice stream and Jakobshavn Isbrae) slide at velocities  $>400 \text{ m yr}^{-1}$  [Truffer and Echelmeyer, 2003], and the most thoroughly modeled ice stream of the Laurentide ice sheet (Hudson Strait Ice Stream) probably moved even faster [Marshall and Clarke, 1997b]. The part of the Illinoian ice sheet that advanced over the outwash of this study was considerably more sluggish and thus is a poor

candidate for an ice stream. This conclusion and the lack of bed deformation indicate basal conditions quite different from those attributed to lobes of the late-Wisconsin Laurentide ice sheet in this area, which are thought to have moved rapidly on shearing sediments and to have been very thin with low surface slopes [e.g., Clark, 1994; Jenson *et al.*, 1996].

[41] Future work on this method for estimating sliding velocity should include laboratory experiments in which temperate ice is slid over a sand bed containing clasts of different sizes. Such experiments would provide a definitive test of the method. Although no device is available that meets the necessary requirements for size, temperature control, shearing displacement, and stress regulation, efforts are underway to build a device for study of this and other aspects of glacier sliding.

[42] Application of this technique at other locations will depend on whether similar bedding planes with plowing structures can be identified. Although at locations elsewhere in Illinois, glacial sediments have been cemented by carbonates [Clark and Hansel, 1989], such cementation is rare. Therefore an important question is whether plowing structures can be exposed successfully in sediments that are unlithified. Field observations of prows on recently deglaciated surfaces [Boulton, 1976; Hart, 1995] and of grooves, manifested as sole markings in the geologic record [Westgate, 1968; Ehlers and Stephan, 1979; Shaw, 1982, 1987], indicate that such features are common. Efforts to apply this method should be focused where advances of ice sheets have left basal tills overlying outwash [e.g., Shaw, 1982, 1987]. The large hydraulic diffusivity of sand and gravel ensures that excess pore pressure due to clast plowing, which complicates estimation of plowing resistance, did not develop. The outwash surface (or the sole of the overlying till) would need to be exposed over an area probably  $>10 \text{ m}^2$  to find a sufficient number of clasts that plowed.

## 6. Conclusions

[43] We have estimated the sliding velocity of a past ice sheet using structures in the sedimentary record to determine the size distribution of clasts that plowed. This size distribution provides an estimate of velocity that depends only on the rheology of ice and on the thermodynamic properties of ice and clasts.

[44] In the vicinity of Peoria the Illinoian ice sheet slid over its bed at a velocity less than  $\sim 170 \text{ m yr}^{-1}$ . A fluidity parameter for normal temperate ice yields an estimate of  $140\text{--}168 \text{ m yr}^{-1}$ ; a fluidity parameter appropriate for basal ice yields a better estimate of  $60\text{--}72 \text{ m yr}^{-1}$ . Sliding velocity may have been even smaller, however, owing to the poorly known and neglected effects of solutes and of friction between debris in ice and plowing clasts. Thus this part of the ice sheet was likely not an ice stream. Effective normal stress on the sand and gravel bed was greater than  $\sim 210 \text{ kPa}$ , as indicated by the size distribution of clasts, and  $<1160 \pm 555 \text{ kPa}$ , as indicated by preconsolidation tests. Bed shear strength was high ( $>145 \text{ kPa}$ ) and indicates that the bed likely did not deform pervasively in shear, consistent with intact primary structures preserved within it. The low basal velocity and lack of pervasive bed deformation

are in contrast to the fast flow and bed deformation advocated for some lobes of the southern margin of the late-Wisconsin Laurentide ice sheet.

[45] As models of past ice sheets increase their fidelity, the need for better data to test and tune such models increases also. Because basal motion is largely responsible for fast glacier flow but difficult to incorporate in models, independent estimates of basal velocity are worth seeking. Our technique can be applied, in principle, wherever an ice sheet advanced over outwash and the bed surface has not been disturbed. Carefully exposing outwash buried by basal till would be laborious but potentially rewarding; there are no alternative methods for estimating sliding velocity from the geologic record.

[46] **Acknowledgments.** We thank A. Hansel for providing helpful information regarding the Glendale School section and the editors and anonymous reviewers for suggesting improvements. This work was supported in part by NSF grant OPP-9725360.

## References

- Alley, R. B. (1989), Water-pressure coupling of sliding and bed deformation, II, Velocity-depth profiles, *J. Glaciol.*, *35*, 119–129.
- Boulton, G. S. (1976), Origin of glacially fluted surfaces: Observations and theory, *J. Glaciol.*, *17*, 287–309.
- Boulton, G. S., and K. E. Dobbie (1993), Consolidation of sediments by glaciers: Relations between sediment geotechnics, soft-bed glacier dynamics and subglacial ground-water flow, *J. Glaciol.*, *39*, 26–44.
- Boulton, G. S., and R. C. A. Hindmarsh (1987), Sediment deformation beneath glaciers: Rheology and geological consequences, *J. Geophys. Res.*, *92*, 9059–9082.
- Bradley, W. C., and A. I. Mears (1980), Calculations of flows needed to transport coarse fraction of Boulder Creek alluvium at Boulder Creek, Colorado, *Geol. Soc. Am. Bull.*, *91*, 1057–1090.
- Brown, N. E., B. Hallet, and D. B. Booth (1987), Rapid soft bed sliding of the Puget glacial lobe, *J. Geophys. Res.*, *92*, 8985–8997.
- Campanella, R. G., P. K. Robertson, and D. Gillespie (1983), Cone penetration testing in deltaic soils, *Can. Geotech. J.*, *20*, 23–35.
- Casagrande, A. (1936), The determination of the preconsolidation load and its practical significance, in *Proceedings, First International Conference on Soils Mechanics and Foundation Engineering*, vol. 3, pp. 60–64, Harvard Univ. Press, Cambridge, Mass.
- Chaney, R. C., and K. R. Demars (Eds.) (1985), *Strength Testing of Marine Sediments: Laboratory and In-Situ Measurements, Spec. Publ. 883*, Am. Soc. for Test. and Mater., Philadelphia, Pa.
- Clark, P. U. (1994), Unstable behavior of the Laurentide Ice Sheet over deforming sediment and its implications for climate change, *Quat. Res.*, *41*, 19–25.
- Clark, P. U., and A. K. Hansel (1989), Clast ploughing, lodgement and glacier sliding over a soft glacier bed, *Boreas*, *18*, 201–207.
- Clark, P. U., R. B. Alley, and D. Pollard (1999), Northern Hemisphere ice-sheet influences on global climate change, *Science*, *286*, 1104–1111.
- Clarke, G. K. C., S. J. Marshall, C. Hillaire-Marcel, G. Bilodeau, and C. Veiga-Pires (1999), A glaciological perspective on Heinrich events, in *Mechanisms of Global Climate Change at Millennial Time Scales, Geophys. Monogr. Ser.*, vol. 112, edited by P. U. Clark, R. S. Webb, and L. D. Keigwin, pp. 243–262, AGU, Washington, D. C.
- Cohen, D. (2000), Rheology of ice at the bed of Engabreen, Norway, *J. Glaciol.*, *46*, 611–621.
- Costa, J. E. (1983), Paleohydraulic reconstruction of flash-flood peaks from boulder deposits in the Colorado Front Range, *Geol. Soc. Am. Bull.*, *94*, 986–1004.
- Das, B. M. (1994), *Principles of Geotechnical Engineering*, 672 pp., PWS Publ., Boston, Mass.
- Drake, L. D., and R. L. Shreve (1973), Pressure melting and regelation of ice by round wires, *Proc. R. Soc. London, Ser. A*, *332*, 51–83.
- Ehlers, J., and H.-J. Stephan (1979), Forms at the base of till strata as indicators of ice movement, *J. Glaciol.*, *22*, 345–355.
- Follmer, L. R., E. D. MacKay, J. A. Lineback, and D. L. Gross (1979), *Wisconsinan, Sangamian, and Illinoian Stratigraphy in Central Illinois*, 139 pp., *Guideb. 13*, Ill. State Geol. Surv., Champaign.
- Freeze, R. A., and J. A. Cherry (1979), *Groundwater*, 604 pp., Prentice-Hall, Old Tappan, N. J.
- Hallet, B. (1976), The effect of subglacial chemical processes on sliding, *J. Glaciol.*, *17*, 209–221.

- Hansel, A. K., and W. H. Johnson (1996), *Wedron and Mason Groups: Lithostratigraphic Reclassification of Deposits of the Wisconsin Episode, Lake Michigan Lobe Area*, *Bull. 104*, 116 pp., Dept. of Nat. Resour. Ill. State Geol. Surv., Champaign.
- Harrison, W. (1958), Marginal zones of vanished glaciers reconstructed from the pre-consolidation-pressure values of overridden silts, *J. Geol.*, *66*, 72–95.
- Hart, J. K. (1995), Recent drumlins, flutes and lineations at Vestari-Hagafellsjökull, Iceland, *J. Glaciol.*, *41*, 596–606.
- Hooyer, T. S., and N. R. Iverson (2002), Flow mechanism of the Des Moines lobe of the Laurentide ice sheet, *J. Glaciol.*, *48*, 575–586.
- Iverson, N. R. (1999), Coupling between a glacier and a soft bed: II. Model results, *J. Glaciol.*, *45*, 41–53.
- Iverson, N. R., D. Cohen, T. S. Hooyer, U. H. Fischer, M. Jackson, P. L. Moore, G. Lappégard, and J. Kohler (2003), Effects of basal debris on glacier flow, *Science*, *301*, 81–83.
- Jenson, J. W., D. R. MacAyeal, P. U. Clark, C. L. Ho, and J. C. Vela (1996), Numerical modeling of subglacial sediment deformation: Implications for the behavior of the Lake Michigan Lobe, Laurentide Ice Sheet, *J. Geophys. Res.*, *101*, 8717–8728.
- Lambe, T. W., and R. Whitman (1969), *Soil Mechanics*, 553 pp., John Wiley, Hoboken, N. J.
- Larsen, E., R. Sandven, H. Heyerdahl, and S. Hernes (1995), Glacial geological implications of preconsolidation values in sub-till sediments at Skorgenes, western Norway, *Boreas*, *24*, 37–46.
- Lliboutry, L. (1979), Local friction laws for glaciers: A critical review and new openings, *J. Glaciol.*, *23*, 67–95.
- Lliboutry, L., and P. Duval (1985), Various isotropic and anisotropic ices found in glaciers and polar ice sheets and their corresponding rheologies, *Ann. Geophys.*, *3*, 207–224.
- Lliboutry, L., and C. Ritz (1978), Ecoulement permanent d'un fluide visquesux non linéaire (corps de Glen) autour d'une sphère parfaitement lissé, *Ann. Geophys.*, *34*, 133–146.
- Marshall, S. J., and G. K. C. Clarke (1997a), A continuum mixture model of ice stream thermomechanics in the Laurentide Ice Sheet: 1. Theory, *J. Geophys. Res.*, *102*, 20,599–20,613.
- Marshall, S. J., and G. K. C. Clarke (1997b), A continuum mixture model of ice stream thermomechanics in the Laurentide Ice Sheet: 2. Application to the Hudson Strait Ice Stream, *J. Geophys. Res.*, *102*, 20,615–20,637.
- Mickelson, D. M., L. J. Acomb, and T. B. Edil (1979), The origin of preconsolidated and normally consolidated tills in eastern Wisconsin, U.S.A., in *Moraines and Varves*, edited by C. Schlucter, pp. 179–187, A. A. Balkema, Brookfield, Vt.
- Nye, J. F. (1968), Theory of regelation, *Philos. Mag.*, *8*, 1249–1266.
- Paterson, W. S. B. (1994), *The Physics of Glaciers*, 3rd ed., 480 pp., Pergamon, New York.
- Prior, J. C. (1991), *Landforms of Iowa*, 153 pp., Univ. of Iowa Press, Iowa City.
- Senneset, K., and N. Janbu (1985), Shear strength parameters obtained from static cone penetration tests, in *Strength Testing of Marine Sediments: Laboratory and In-Situ Methods*, edited by R. C. Chaney and K. R. Demars, pp. 41–54, Am. Soc. of Test. and Mater., Philadelphia, Pa.
- Shaw, J. (1982), Melt-out till in the Edmonton area, Alberta, Canada, *Can. J. Earth Sci.*, *19*, 1548–1569.
- Shaw, J. (1987), Glacial sedimentary processes and environmental reconstruction based on lithofacies, *Sedimentology*, *34*, 103–116.
- Stokes, C. R., and C. D. Clark (2002), Are long subglacial bedforms indicative of fast glacier flow, *Boreas*, *31*, 239–249.
- Thomason, J. F., and N. R. Iverson (2003), Flow mechanism of ice sheets on un lithified sediment: Plowing of clasts at the ice-bed interface, *GSA Abstr.*, *35*, Ann. Meet. Suppl., Abstract 122-9.
- Touloukian, Y. S., W. R. Judd, and R. Roy (1981), *Physical Properties of Rocks and Minerals*, 548 pp., McGraw-Hill, New York.
- Truffer, M., and K. Echelmeyer (2003), Of isbrae and ice streams, *Ann. Glaciol.*, *36*, 66–72.
- Tulaczyk, S., B. Kamb, and H. Engelhardt (2001), Estimates of effective stress beneath a modern West Antarctic ice stream from till preconsolidation and void ratio, *Boreas*, *30*, 101–114.
- Verruijt, A., F. L. Beringen, and E. H. de Leeuw (Eds.) (1982), *Penetration Testing*, vol. 1, A. A. Balkema, Brookfield, Vt.
- Walder, J. S. (1982), Stability of sheet flow of water beneath temperate glaciers and implications for glacier sliding, *J. Glaciol.*, *28*, 273–293.
- Westgate, J. A. (1968), Linear sole markings in Pleistocene till, *Geol. Mag.*, *105*, 501–505.

T. S. Hooyer, Wisconsin Geological and Natural History Survey, University of Wisconsin, 3817 Mineral Point Road, Madison, WI 53705, USA. (tshooyer@facstaff.wisc.edu)

N. R. Iverson, Department of Geological and Atmospheric Sciences, 253 Sciences I, Iowa State University, Ames, IA 50011, USA. (niverson@iastate.edu)